Electronic Supplementary Material (ESI) for ChemComm.

Supporting Information

Tailor-Made Oxide Architectures Attained by Molecularly Permeable Metal-Oxide Organic Hybrid Thin Films

Debabrata Sarkar, Dereje Hailu Taffa, Sergey Ishchuk, Ori Hazut, Hagai Cohen, Gil Toker, Micha Asscher, and Roie Yerushalmi

MLD process:

Ti-EG films were prepared using $TiCl_4$ (Acros, 99.9%) and ethylene glycol (Aldrich, > 99%). Ultra pure water (>18MΩ, ELGA purification system) was used for ALD of TiO_2. Ultrahigh purity Ar gas was used as the carrier gas in viscous flow reactor and for purge between reactant exposures. MLD films were prepared by dosing the reactant precursors into Ar carrier gas. The duration of precursor dosing was controlled using computer controlled pneumatic valves (EG 70 sec, Ar purge 30 sec, $TiCl_4$ 0.3 sec, Ar purge 9 sec). A steady state pressure of 2.1×10^{-1} mBar was maintained during the process. For MLD process the water and EG precursor chamber temperatures were set to 40 and 80°C, respectively and the sample reactor temperature was set to 100°C. The films were prepared on various substrates such as Pt coated Si wafers, quartz slides, and ITO. Prior to film formation the substrates were cleaned using UVOCS Ozone cleaning system for 10 min. Ti-EG samples of different thickness ranging 10-60 cycles were prepared. Films were thermally annealed at the specified temperatures for 30 minutes. For thermal anneal of the films, the oven temperature was equilibrated to the desired temperature prior to sample loading to avoid kinetic effects of temperature ramp.

Electrochemical measurements

Electrochemical experiments were carried out using Biologic SP 300 potentiostat interfaced with a personal computer running ECLab software for Windows (Biologic Instruments, France). A standard three electrode electrochemical cell with a Pt mesh counter electrode and a Ag/AgCl (3M NaCl) reference electrode were used. Pt electrodes coated with Ti-EG or TiO_2 films with a geometric area of 0.5 cm^2 served as working electrodes. Electrolyte was 0.1 M KCl with 2mM $K_3[Fe(CN)_6]$ (Aldrich). pH was adjusted with 0.1M HCl or 0.1M NaOH solutions. Cyclic voltammetry was performed at a scan rate of 100 mV/s. The electrochemical impedance measurements were obtained using the same setup with 10 mV ac signal amplitude and frequency range 10^5 to 10^{-2} Hz. The applied potential was set to 0.22V.

Thin Film Surface area analysis using CO-TPD:

Surface area measurements were performed in a UHV chamber (base pressure of $3*10^{-10}$ Torr) equipped with standard surface characterization tools and a residual gas analyser (SRS- RGA 200) for Temperature Programmed Desorption (TPD) analysis. The sample was cooled to 50K using closed cycle He cryostat and CO was introduced and adsorbed on the surface through a variable leak valve. Following CO exposure, the sample was heated resistively and CO TPD signal was recorded. The integrated desorption signal and total CO uptake is plotted against CO exposure (measured in Langmuirs: $1L=10^{-6}$ torr*sec) for a Ti-EG sample and a reference, pristine SiO_2/Si(100) sample. The experimental data is fitted using the Langmuir equation assuming an adsorption curve for CO based on the simple coverage dependent sticking probability often considered as Langmuir adsorption mechanism: $S(\theta)=S_o(1-\theta)$, where S_o equals unity at the adsorption temperature used in the measurements.[1] The calculated curve is given by the dashed line through the data points in Fig. 1d. Ti-EG films, 40 cycles were prepared on SiO_2/Si(100) at 100 °C and annealed under air at 600 °C for 30 minutes. CO TPD data show that Ti-EG sample surface area is increased by a factor of 2.6±0.4 compared to the reference sample under identical conditions.

Work Function Measurements by CREM-XPS.

Measurements were performed on a Kratos AXIS-Ultra DLD spectrometer, using a monochromatic Al kα source at low power, 15-75 W. The analysis chamber base pressure was $5 \cdot 10^{-10}$ torr. Detection pass-energies ranged between 20 and 80 eV. Our experimental protocol particularly addresses the requirement for reliable elimination of beam induced electrostatic changes, following procedures presented in detail elsewhere.[2] This procedure is based on using an *in-situ* reference for work-function (WF) measurement of the bare surface, before applying any x-ray irradiation, which is followed by repeated scans of the core and valence-electron signals, as well as repeated WF measurements. This enables reliable evaluation of both sample charging and irreversible surface modifications. In addition, the response to electron flood gun (eFG) irradiation was studied under 1.8 A filament current and grid bias of 3.3 V, providing an in-situ reference for layer dielectric properties and charging tendencies in particular.[3,4]

	WF (eV)	**VBM (eV)**	**Δ_{eFG} (meV)**
Bare Pt	4.91	0.00	-
Undoped Ti-EG/Pt	4.85	2.80	40
Fe-doped Ti-EG/Pt	4.89	2.38	40
Ni-doped Ti-EG/Pt	4.79	2.48	30

Table S1. Work-function (WF) of non-irradiated samples, corrected valence band maximum (VBM) referenced to Pt, and XPS line-shifts induced by eFG (Δ_{eFG}). The substrate shifts under eFG irradiation, given in the last column, were fully reversible.

Measured WF values are listed in table S1, showing small variations only (within ~100 meV) among the samples studied. This could be attributed to de-wetting of the annealed film on the Pt substrate at the high anneal temperature (750 ^{o}C) used here for doping. In addition, valence band maximum energies (VBM) were corrected for beam-induced changes and their associated electrostatic shifts. VBM values are given in reference to the Pt Fermi energy level. Since the VB spectra are masked by Pt signals (measured also by He-I and He-II UPS, not shown), hampering the direct extraction of the VBM values, an indirect approach was applied by measuring the shifts in the Ti and O core electron levels, thus obtaining the *relative* changes in surface potentials for the doped and un-doped samples.

The relative positions are then transformed to an absolute energy scale using a reference set of Ti-EG samples, prepared on a SiO_2/Si substrate, where the Ti-EG related VBM could be identified spectrally. Corresponding band diagrams were deduced by combining optically-derived band-gap energies (BG), with the VBM values obtained as described here (see Fig. 2d).

The response to controlled negative charging *via* chemically resolved electrical measurements (CREM)[3] provided complementing information regarding the dielectric properties of the studied overlayers.[3] CREM measurements showed only a small potential buildup across the annealed Ti-EG overlayer for all samples under electron source application, below 50 meV (Δ_{eFG} values in table S1). Similar values were obtained for the various overlayer elements for each sample.

X-ray diffraction (XRD) Analysis: Photocatalytic Degradation

The crystal phase of the undoped and Fe, Ni-doped Ti-EG films annealed at 750˚ C were characterized by X-ray diffraction (XRD) with a Rigaku SmartLab X-ray diffractometer (Cu Kα radiation (λ = 1.54 Å), 3KW). Continuous theta-2theta scans and 2theta grazing incidence XRD (GIXRD) for thin film analysis scans were performed. The angle of incidence α was set to 0.8°.

XRD patterns of un-doped Ti-EG, Fe-doped and Ni-doped Ti-EG films after anneal at 750˚ C are presented in **Fig. S5** and **table S2**.

XRD data confirm the formation of crystalline anatase phase TiO_2 in all films. For un-doped film, diffraction peaks around 2θ=25.35˚ and 48.1˚ are assigned to formation of (101) and (200) phase of anatase TiO_2 with space group $I4_1/amd$ (ICDD 01-075-2552).

For Ni-doped Ti-EG films additional peak was detected at 2θ=27.43˚ which is assigned to TiO2 rutile phase, in-line with previous reports showing the formation of rutile phase for Ni-doped TiO_2.[5] Additional peak at 2θ=33.10˚ is assigned to nickel-titanium oxide phase, in-line with previous report by Mariana et al. showing nickel-titanium oxide peak for high Ni doping levels. [RSC Adv., 2014, 4, 4308–4316] No other peaks of metallic nickel or nickel oxide phases were detected. Finally, the slight shift of anatase (101) peak position from 25.35˚ to 25.42˚, owing to the smaller atomic radii of Ni compared to Ti suggest substitutional doping.

For Fe-doped Ti-EG films only the anatase phase could be observed with a slight shift of the anatase (101) peak position from 25.35˚ to 25.45˚, owing to the smaller atomic radii of Fe compared to Ti suggest substitutional doping as well.[6,7] No additional XRD peaks could be observed for Fe-doped Ti-EG films.

Sample	2 θ (deg)	Phase	FWHM	Plane	d spacing (A˚)
Undoped Ti-EG	25.35	anatase	1.031	101	3.509
	48.14	anatase	1.462	200	1.888
Fe doped Ti-EG	25.45	anatase	1.04	101	3.497
	48.19	anatase	1.473	200	1.886
Ni doped Ti-EG	25.42	anatase	1.105	101	3.501
	27.43	rutile	1.217	110	3.249
	33.10	$NiTiO_3$		104	2.702
	48.15	anatase	2.23	200	1.888

Table S2. Summary of XRD data for un-doped, Fe-doped, and Ni-doped Ti-EG film annealed at 750 ˚C.

XPS Surface analysis.

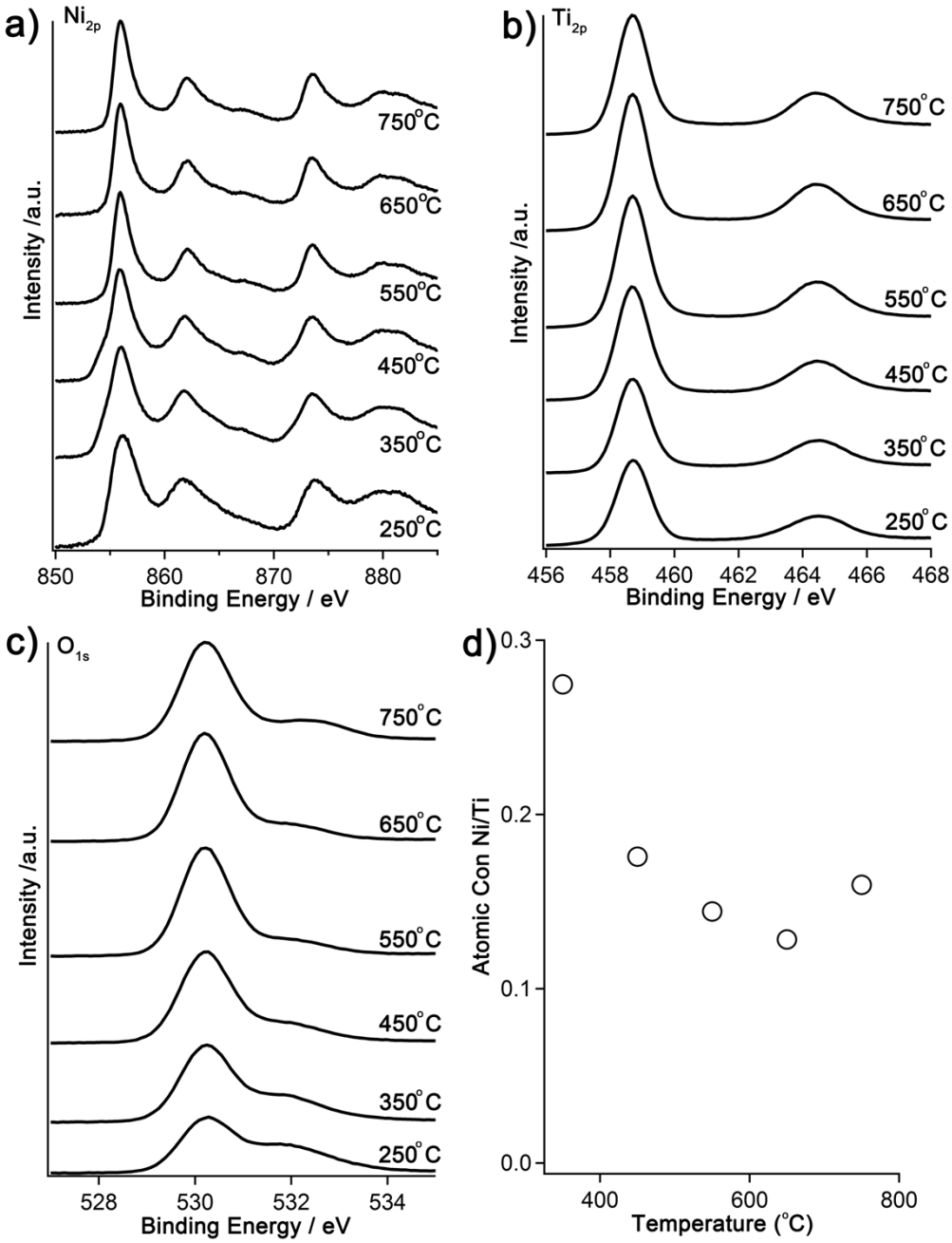

Fig. S1. XP spectra for Ni-doped Ti-EG film at selected annealing temperatures.

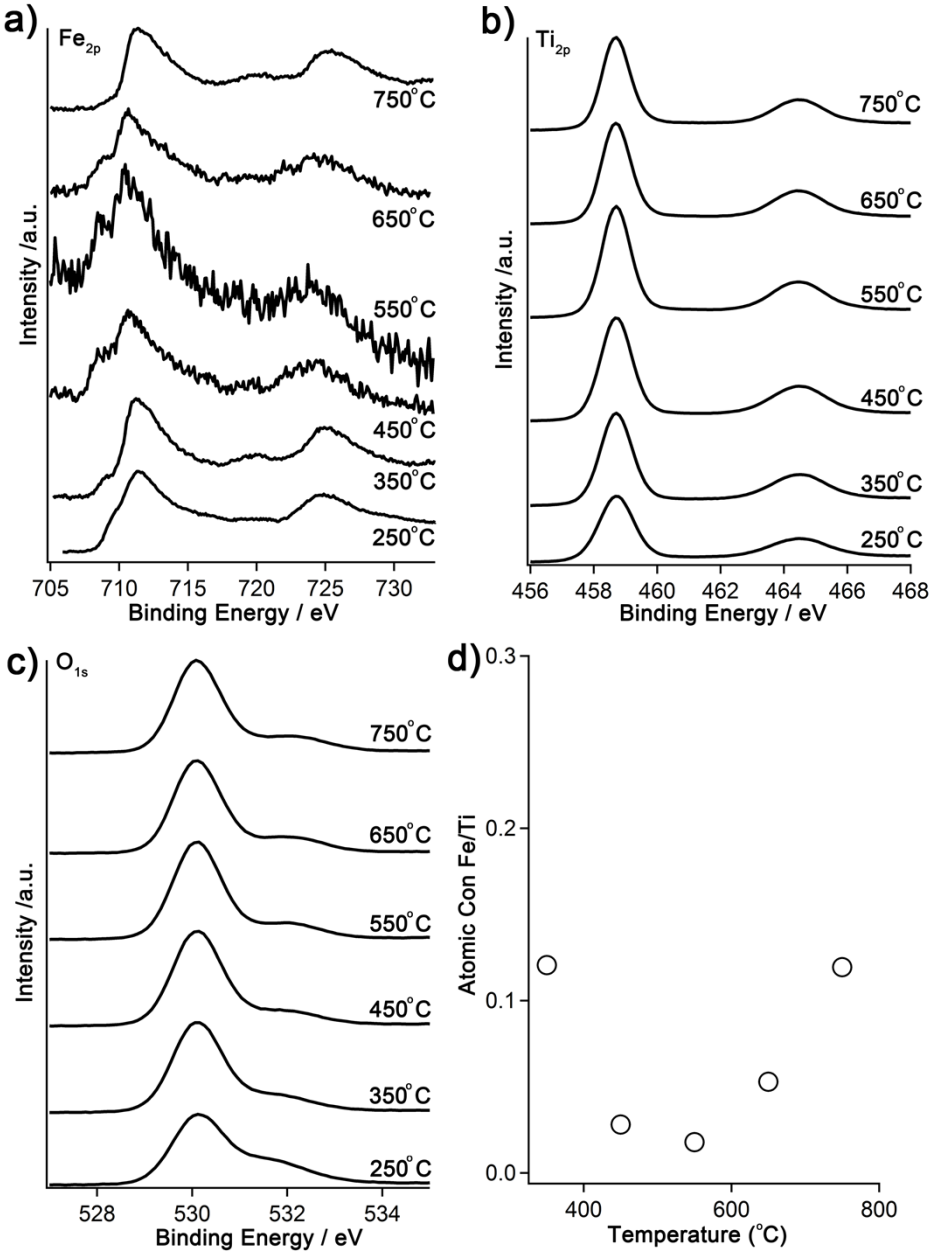

Fig. S2. XP spectra for Fe-doped Ti-EG film at selected annealing temperatures.

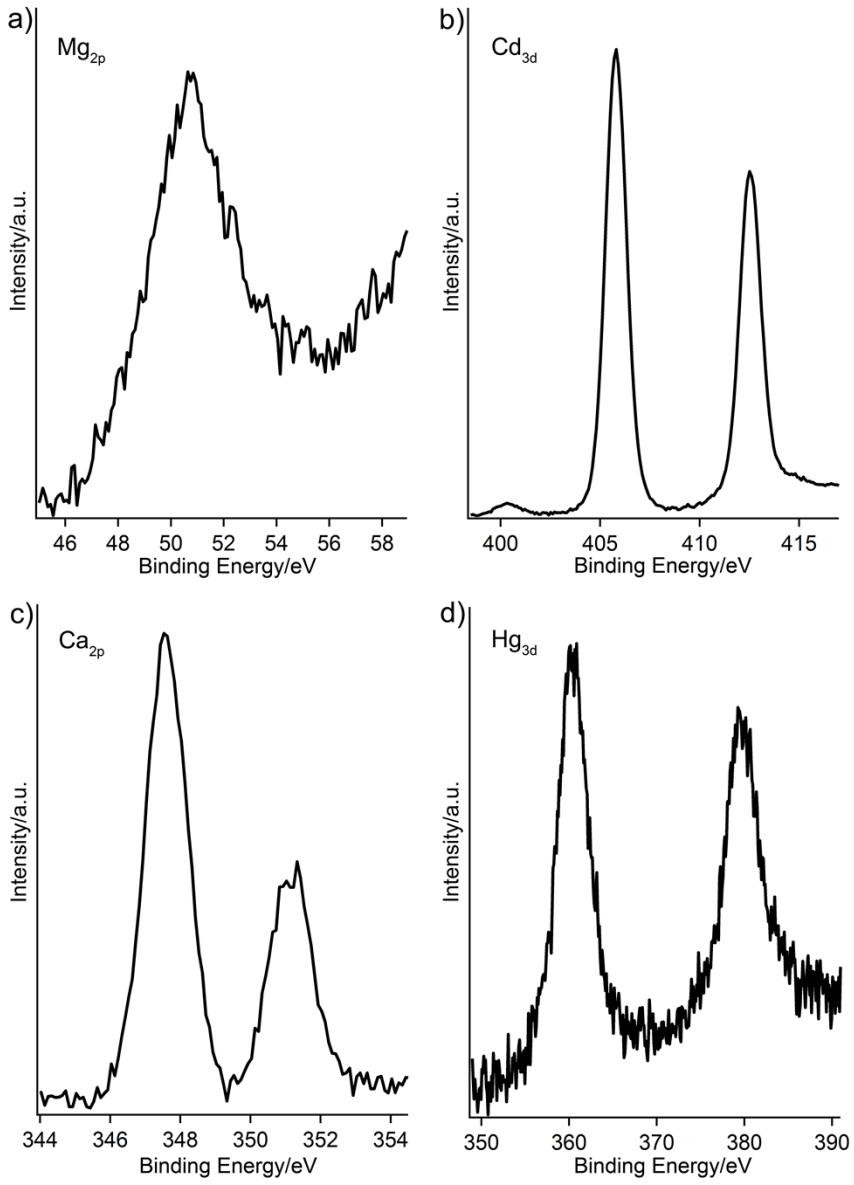

Fig S3. XP spectra of Ti-EG films with cations adsorbed from aqueous solutions. (a) $Mg(NO_3)_2$ 1mM, (b) $Cd(NO_3)_2$ 1mM, (c) $Ca(NO_3)_2$ 1mM, (d) $HgSO_4$ 0.01mM. Ti-EG films prepared at 100 °C, 40 cycles and annealed at 250 °C prior to soaking in the respective cation solution.

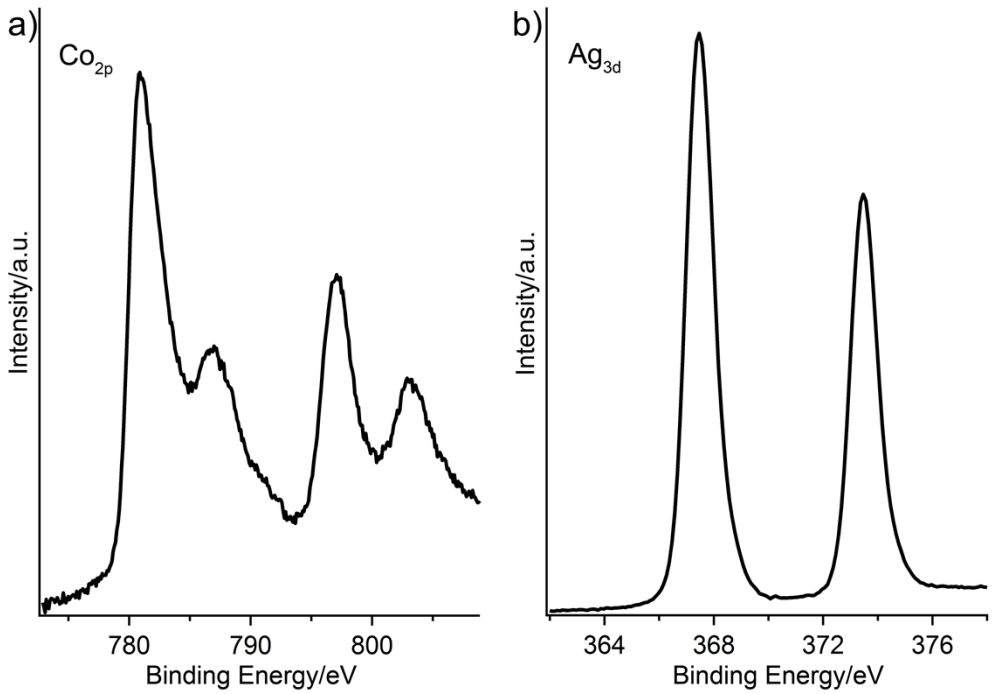

Fig S4. XP spectra of Ti-EG films with cations adsorbed from Acetonitrile solutions. (a) Co(acac) 0.18M, (b) Ag(acac) 0.02M. Ti-EG films prepared at 100 °C, 40 cycles and annealed at 750 °C after soaking in the respective cation solution.

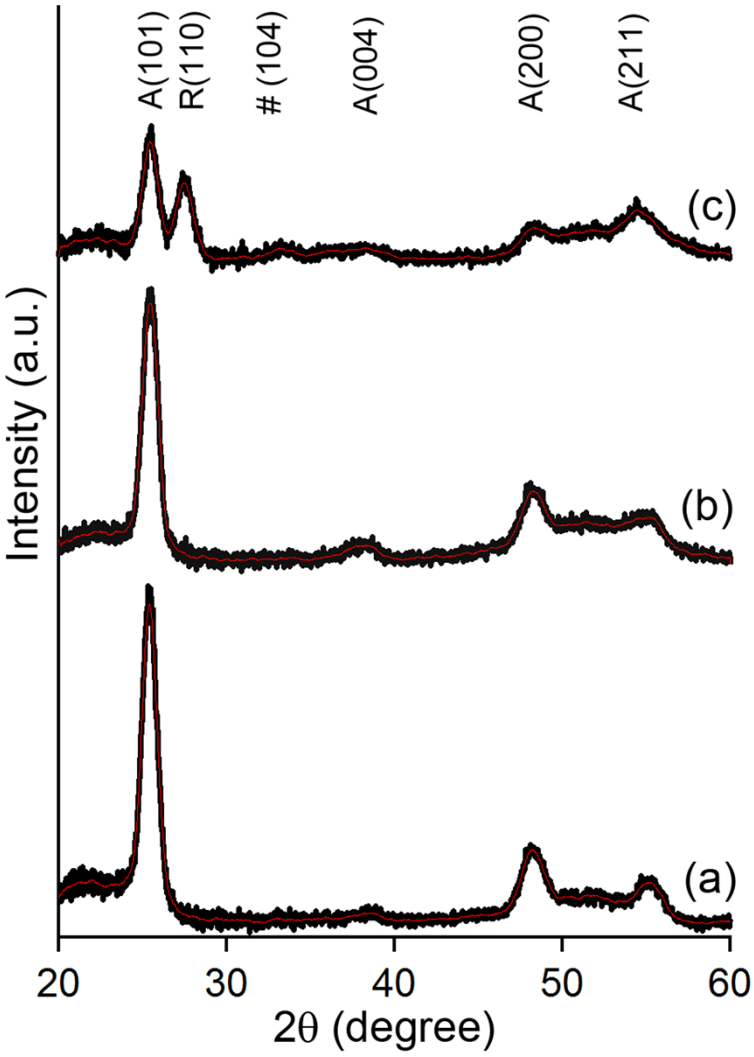

Fig S5. X-ray diffraction patterns of (a) undoped, (b) Fe doped and (c) Ni doped Ti-EG film annealed at 750˚ C. A for anatase, R for rutile and # for $NiTiO_3$.

References

1 R. I. Masel, Principles of Adsorption and Reaction on Solid Surfaces, Wiley series in chemical engineering, J. Wiley & Sons, New York, 1996.

2 Y. Itzhaik, G. Hodes and H. Cohen, *J. Phys. Cem. Lett.,* 2011, **2**, 2872.

3 H. Cohen, *Appl. Phy. Lett.,* 2004, **85**,1271.

4 I. D. Mor, A. Hatzor, A. Vaskevich, T. van der B. Moav, A. Shanzer, I. Rubinstein and H. Cohen, *Nature*, 2000, **406**, 382.

5 J. Tian, H. Gao, H. Deng, L. Sun, H. Kong and P. Yang, J. Chu, *J. Alloys and Comp.*, 2013, **581**, 318.

6 M. Gharagozlou and R.Bayati, *Ceram. Inter.*, 2014, **40**, 10247.

7 R. Khan and T. J. Kim, *J. Hazard. Mater.,* 2009, **163**, 1179.